Antarctic Science 16 (2): 205–213 (2004) © Antarctic Science Ltd Printed in the UK DOI: 10.1017/S0954102004001919

Glaciological characteristics of Institute Ice Stream using remote sensing

TED SCAMBOS*, JENNIFER BOHLANDER, BRUCE RAUP and TERRY HARAN

National Snow and Ice Data Center, CIRES, UCB Box 449, 1540 30th Street, University of Colorado, Boulder, CO 80309, USA
**teds@icehouse.colorado.edu*

Abstract: We assess the ice flow of Institute Ice Stream (IIS; 81.5°S, 75°W) and the adjacent Ronne Ice Shelf using satellite images and geophysical parameters from recent continent-wide compilations. Landsat image pairs from the 1980s and 1990s are used to determine ice velocity. Peak speed is 398 ± 10 m a^{-1}. Several mappings using images spanning an eleven-year period indicate this speed and the pattern of ice flow throughout the mapped portion of the stream is constant to within ± 20 m a^{-1}. Combining catchment extent (141 700 km^2) with surface accumulation, mass input to IIS is 25.1 ± 2 Gt a^{-1}. Mean ice thickness across the grounding line is 1177 m. Mass flux to the Ronne Ice Shelf, determined from these values and our velocity profile, is 22.7 ± 2 Gt a^{-1}. Topographic mapping using photoclinometry, coupled with ice thickness and ice velocity, permits an assessment of driving force versus flow speed. This indicates wide variations in basal resistance. Despite evidence of present-day near-balance and constant speed in the ice stream trunk, a recent change in outflow is implied by folding of shelf streaklines near Korff Ice Rise. This may be a result of changing shelf thickness or erosion of Doake Ice Rumples.

Received 27 January 2003, accepted 3 October 2003

Key words: Antarctica, glaciology, ice streams, Institute Ice Stream, mass balance, remote sensing

Introduction

On the basis of width and outflow, Institute Ice Stream (IIS) it is among the largest glaciers in Antarctica, and therefore, in the world (Fig. 1). Early satellite photography (1961 "Argon" images from the US Defense Intelligence Satellite Program) indicated the presence of a large outlet glacier between the Skytrain Ice Rise and an ice rise to the south-east. However, as this imagery was initially held secret, the ice stream was not identified until airborne radar mapping in the late 1970s (Drewry 1983). The glacier was given its name to commemorate the contribution of the Scott Polar Research Institute to early exploration of the Ronne area (Alberts 1995). In 1976, and again in 1986, Landsat and AVHRR (Advanced Very High Resolution Radiometer) satellite image mosaics of the Filchner–Ronne Ice Shelf (FRIS) were compiled, revealing the extent of the trunk and outflow of the IIS (Swithinbank *et al.* 1988). Some early studies that included the IIS (e.g. McIntyre 1986) estimated its basic characteristics. Recently, mass balance and grounding line melting have been determined by interferometric synthetic aperture radar methods (Rignot & Thomas 2002, Rignot & Jacobs 2002). These studies show the IIS to be nearly in balance, with modest subglacial melt rates. We will look at the glacier more closely here, using a combination of Landsat, AVHRR, and MODIS (Moderate Resolution Imaging Spectroradiometer) images, and recent continent-wide compilations of accumulation (Vaughan *et al.* 1999), ice thickness (BEDMAP; Lythe *et al.* 2001), and radar imagery (Radarsat Antarctic Mapping Project, or RAMP, mosaic, and the associated RAMP digital elevation model, the RAMP DEM; Jezek 1999, Liu *et al.* 1999, Jezek *et al.* 1999).

This study demonstrates two things: that IIS is worthy of additional, field-programme research to investigate its basal and grounding area characteristics, and that a substantial amount of knowledge about a glacier may now be gathered purely by remote sensing. Recent advances in the application of satellite remote sensing to glaciology (summarized in Bindschadler 1998) allow a determination of fundamental glaciological parameters for any glacier within reach of satellite coverage. Satellite image pairs now routinely determine surface velocity, either by feature tracking, speckle tracking, or interferometry (e.g. Bindschadler & Scambos 1991, Gray *et al.* 2001). Satellite radar or laser altimetry provide few kilometre resolution maps of surface elevation and slope. Radar and visible/near-infrared images also provide detailed morphology of flow-related surface features (Fahnestock *et al.* 2000). With detailed coverage of elevation and velocity, it is possible to estimate basal melting/freeze-on rates near ice stream grounding lines (Rignot & Jacobs 2002). Passive microwave data may be used to infer accumulation rates, especially when used as an interpolation field for dispersed ground-based measurements (Giovinetto & Zwally 2000, Vaughan *et al.* 1999). Through photoclinometry, elevation maps may be improved using visible-band imagery to yield metre-precision relief maps on the kilometre to decametre scale (Bindschadler & Vornberger 1994, Scambos &

https://doi.org/10.1017/S0954102004001919 Published online by Cambridge University Press

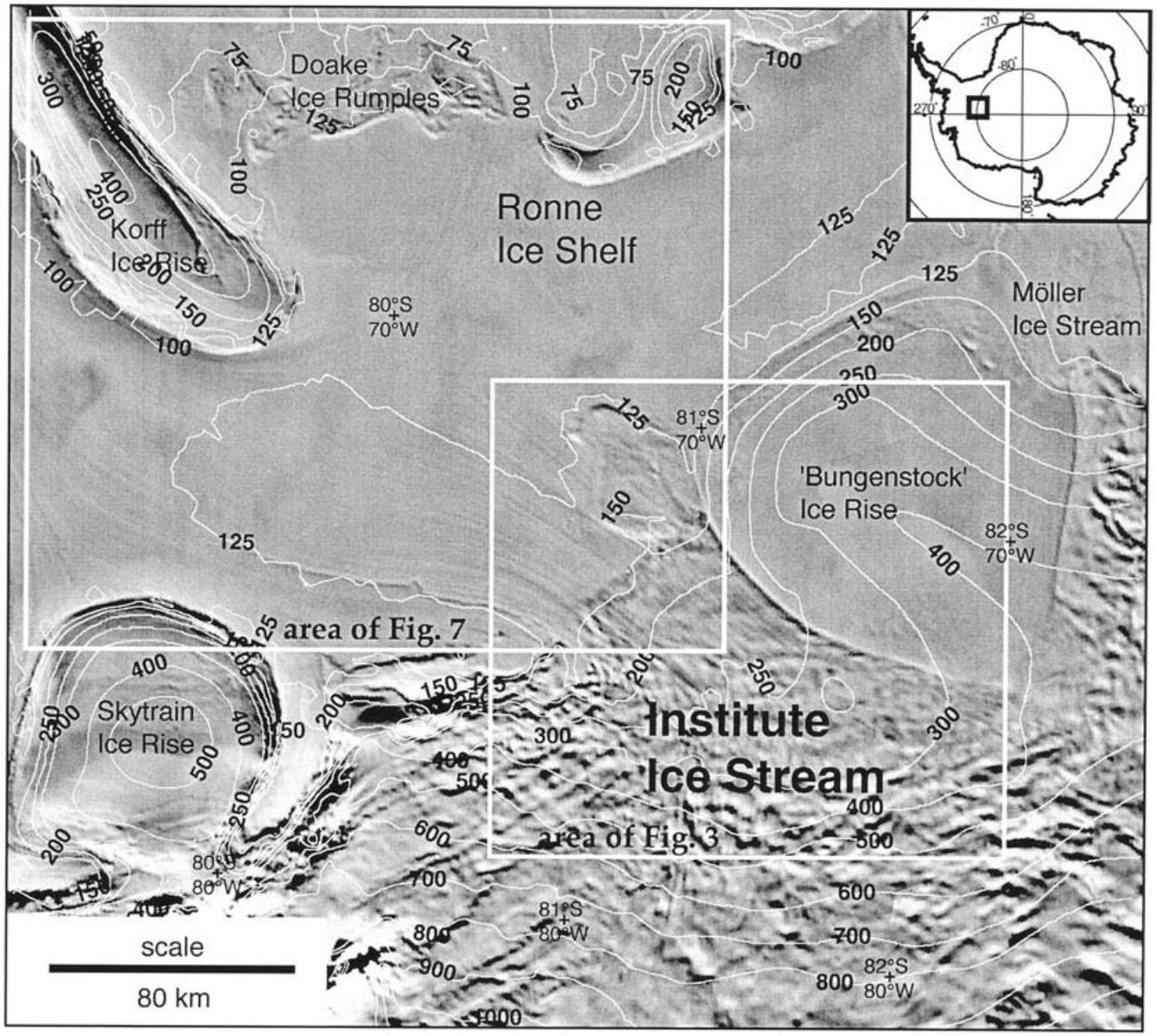


Fig. 1. Enhanced-resolution AVHRR image of Institute Ice Stream and vicinity. Eight AVHRR images acquired between October and December 1996 were used in the composite, producing an image with ~800 m resolution and improved radiometric sensitivity. Illumination direction is from the lower right (20h12–21h00 UTC images). Elevation contours are from the RAMP DEM (Liu *et al.* 1999).

Fahnestock 1998, Scambos & Haran 2002). As the archived record of these data sets lengthens, change detection through repeat remote examination becomes possible.

The results of the remote analysis presented here suggest that the IIS has an unusually low slope and driving stress in its main trunk, and a somewhat larger 'ice plain' area than other FRIS glaciers. Streakline folding on the FRIS in the IIS outflow area implies significant flow changes there. As developed below, the north-eastern side of IIS shows flow and morphologic characteristics reminiscent of the Siple Coast ice streams, though not unknown in the FRIS glaciers as well.

Data sources and remote sensing techniques

Figure 1 is an enhanced-resolution image of IIS region, produced from eight AVHRR images acquired in November–December of 1997 (see Scambos *et al.* 1999 regarding the processing technique). Sub-scenes from the Radarsat Antarctic Mapping Project (RAMP) Antarctic Mapping Mission 1 (AMM-1) synthetic aperture radar (SAR) mosaic identify the active crevasse areas (Fig. 2; see Jezek 1999). Data from the MODIS sensor (Moderate Resolution Imaging Spectrometer) are used to investigate streaklines on the Ronne Ice Shelf. Streaklines, sometimes called 'flowstripes' or 'flowbands', are elongate ridges

https://doi.org/10.1017/S0954102004001919 Published online by Cambridge University Press

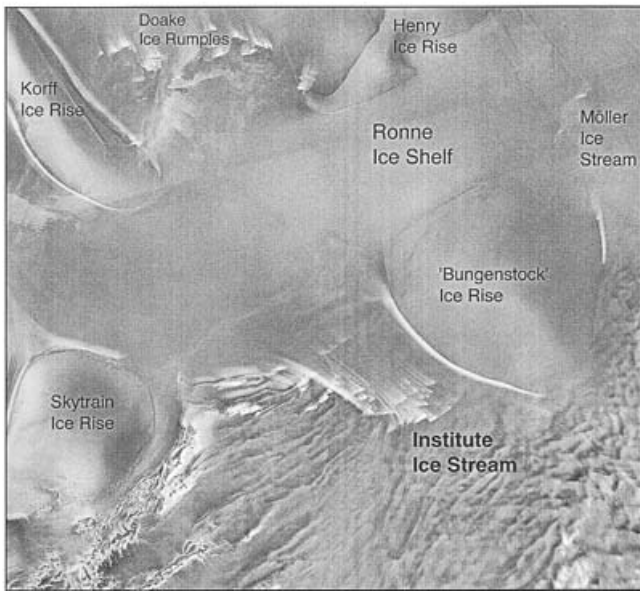


Fig. 2. Radarsat –1 RAMP mosaic subscene, derived from the 125 m-resolution composite (Antarctic Mapping Mission 1). Radarsat mosaic image swaths were acquired between 16 September and 23 October 1997.

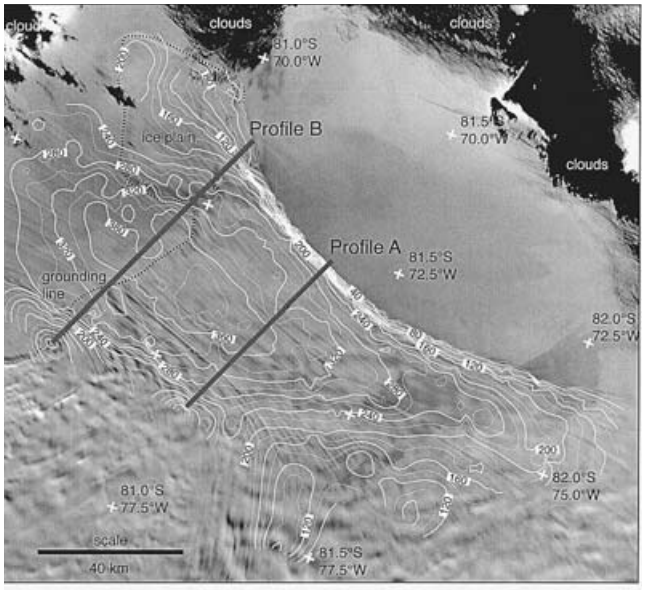


Fig. 3. Ice flow speed contours for IIS trunk plotted over a subscene from a 1989 Landsat 5 image (P190 R120, L5190120008604710). Velocity vectors were determined by measuring pixel displacement of crevasse-related features between this image and a 1986 (P190 R120, L4190120008901510) image. A third image, acquired in 1997 (P188 R120, L5188120009703110), was used to check for velocity changes in selected regions. Contours are masked if greater than 10 km from a displacement measurement.

formed as grounded ice flows over bedrock features; they can persist as surface features as the ice flows out in an ice shelf, serving as an indicator of the stability of flow. The MODIS sensor provides 250-m spatial resolution data with 12-bit radiometric resolution in the visible and near-infrared channels, useful for mapping these faint features and other structures, although images must have a striping artifact removed to make use of their full radiometric sensitivity (Haran *et al*. 2002). Morphologic information is also provided by Landsat Thematic Mapper (TM) images from 1986, 1989, and 1997 (e.g. Fig. 3).

These Landsat TM images were also used to map ice flow velocity and ice strain, and to examine the possibility of changes in flow speed over the 11-year interval they span. We use an image cross-correlation technique to map ice flow by tracking the displacement of crevasse-related features within the trunk of the ice stream (Bindschadler & Scambos 1991, Scambos *et al.* 1992). From the 1986–89 image pair, 7830 vectors were determined. From the 1989–97 pair, 1990 vectors were mapped. These were not as broadly distributed as the earlier vector data set (due to flow distortion of features over the long time separation of the images). The velocity map in Fig. 3 is therefore based on the 1986–89 image pair. For this map, error in average annual flow speed is approximately ± 15 m a^{-1}. Average annual speed error for the eleven-year image pair is ± 5 m a^{-1}.

Elevation data for catchment determination is provided by the RAMP digital elevation model (RAMP DEM; Liu *et al.* 1999, Jezek *et al.* 1999). For the ice stream trunk and ice shelf, this data set was augmented using photoclinometry (sometimes called 'shape from shading'). The method we use applies multiple AVHRR images to determine the slope in a 625-m grid covering the study area. The brightness-to-slope relationship for the images is calibrated by comparison to the RAMP DEM. Regional mean slope and elevation at scales greater than 30 km are still determined by the RAMP DEM, but local slopes and elevations are modified by the image-derived slope field. For the IIS area, we used eight AVHRR images acquired in 1997, with solar illumination azimuths spanning 150 degrees. In a similar application, AVHRR images improved a satellite-radar-altimetry based DEM of the Greenland ice sheet by increasing spatial resolution from ~15 km to ~2 km while maintaining an accuracy of ± 1.5 m (1σ) when compared with airborne laser altimetry profiles (Scambos & Haran 2002). A similar independent validation was not possible here because of a lack of recent high-accuracy elevation profiling (early radar altimetry profiles in the area are too poorly geo-located, and may contain errors due to barometric pressure variations during flights). However, we assume that the images and technique provide a similar improvement here as in Greenland.

Size and shape of Institute Ice Stream

The difference between the two margins of the ice stream is visible in satellite images, particularly in AVHRR (Fig. 1). Crevasse regions, both at the margins and on the trunk, are

https://doi.org/10.1017/S0954102004001919 Published online by Cambridge University Press

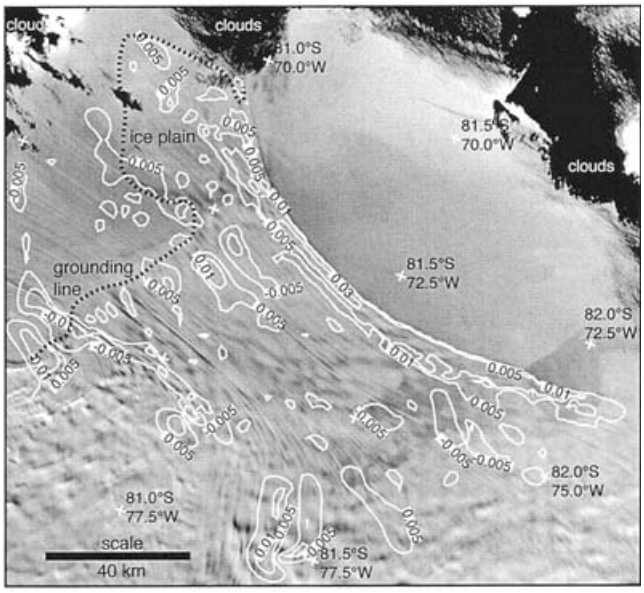


Fig. 4. Shear strain rate determined from the Landsat-derived flow vector field.

visible in SAR (Fig. 2). On the north-eastern side, a distinct, sharp shear margin is indicated by the presence of a narrow band of chaotic crevasses with a sharp boundary to nearly featureless inter-stream ridge (the Bungenstock Ice Rise). In contrast, the western margin is diffuse, with a broader area of shear-related crevassing and streakline convergence, suggesting more lateral influx along it. The IIS trunk is wide and short in comparison to the adjacent ice streams in the FRIS, or the eastern Ross Embayment ice streams, but is better defined by flow (Figs 3 & 4) and surface crevassing than the similarly-proportioned Thwaites Glacier trunk. Trunk width of IIS is 57 km at profile A of Fig. 3, and 82 km at the near-grounding-line profile, B (estimated from the speed profiles and the image morphology). Trunk length, defined here as the distance from the grounding line or ice plain boundary to the onset of streaming flow (discussed later), is approximately 100 km at the centre of the stream.

Several recent studies (Joughin *et al.* 1999, Bamber *et al.* 2000) have shown that outlet glacier flow usually begins in long narrow zones of greater velocity that nearly reach the divides of the ice sheet. However, IIS, as mapped by these papers and in images examined for this study (not shown), appears to have less pronounced channelling of flow in its upper catchment. Using an algorithm developed by USGS in Flagstaff, we determined the catchment area of IIS using the RAMP DEM. We define the catchment as the surface extent of all ice draining through Profile B of Fig. 3. Our result is 141 700 km^2, considerably larger than an earlier estimate by McIntyre (1986) of 105 680 km^2, but less than Rignot & Thomas' (2002) estimate of 166 900 km^2. Differences in our catchment area *versus* the Rignot & Thomas estimate (both of which are based on the RAMP DEM) may be due to the use of slightly different glacier widths at the grounding line. Errors for a catchment determination can be hard to quantify because they stem from errors in the DEM, in some cases very subtle errors.

The catchment borders the southern lobe of the Pine Island Glacier drainage system and the uppermost part of the Bindschadler Ice Stream catchment (formerly ice stream D; Vaughan *et al.* 2001). This implies that the IIS catchment area will vary as the Pine Island glacier system changes. However, this boundary position is likely controlled by the high bedrock topography of Ellsworth Subglacial Highlands, Pirrit Hills, and Whitmore block, and thus would be relatively insensitive to changes on the Pine Island Glacier side. On its southern flank, the IIS catchment borders Foundation and Müller ice streams. The precise location of these boundaries, and the effect of changes in glacier flow, is poorly constrained due to sparse source data for the RAMP DEM.

The grounding line of IIS, determined here by visible-band image analysis and a slope break in the image-enhanced elevation map, is approximately straight and perpendicular to flow along its north-western side, and is similar (within a few kilometres) to the position inferred by Rignot & Jacobs (2002) and Rignot & Thomas (2002). The easternmost portion of the grounding line is an ice plain; the Rignot publications' grounding line follows the slope break at the foot of the glacier and not the perimeter of this lightly grounded, low-slope area. The ice plain is approximately diamond-shaped, with a maximum width of 45 km and a length of 52 km, with gentle undulations within. Similar features are observed at the grounding line of Whillans Ice Stream, and Bindschadler and MacAyeal Ice Streams on the Siple Coast. Other ice streams in the FRIS drainage also show some ice plain areas, but the IIS ice plain is among the largest of these (Swithinbank *et al.* 1988). The RAMP DEM indicates that the ice plain rises about 25 m above the regional shelf level (Fig. 1).

Velocity mapping and mass balance

Flow speed and shear strain rate determined from the 1986–89 Landsat pair are shown in Figs 3 & 4, respectively. Flow direction matches streakline orientation in all mapped areas on the grounded ice, implying that flow direction throughout the grounded portion of the stream has remained unchanged for the last few centuries. Peak velocity of the ice stream is 398 m a^{-1}, in a region just above the grounding line near the centre. Within the trunk, speed variations suggest significant spatial changes in basal resistance (such variations have been called 'sticky spots'). Flow speed drops sharply, and shear strain peaks (maximum of 0.06 a^{-1}), near the south-eastern margin, but speed and strain rate change over a broader zone on the north-western flank. Shear strain is low in the central stream trunk, except for isolated zones on the flanks of sticky spots.

Profiles of ice flow speed further reveal the different

https://doi.org/10.1017/S0954102004001919 Published online by Cambridge University Press

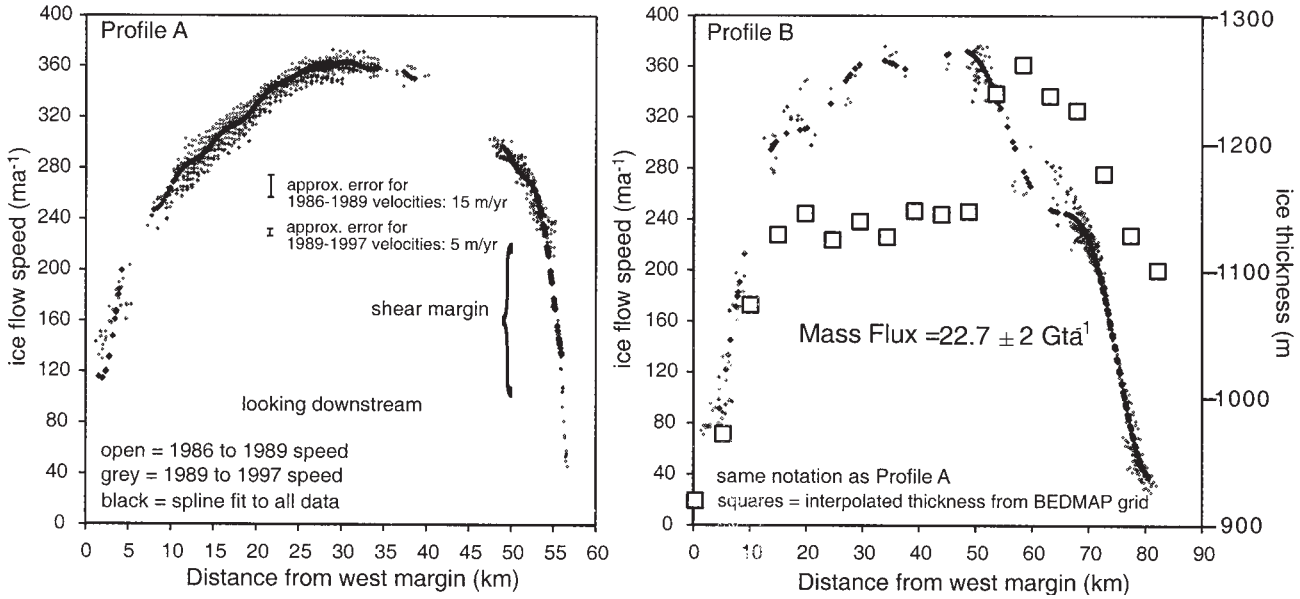


Fig. 5. Across-flow ice speed profiles from the Landsat-derived flow vector field, and ice thickness across the ice stream near its grounding line.

character of the two lateral shear margins (Fig. 5). The south-eastern margin exhibits more concentrated shear and a more distinct boundary with the adjacent ice dome. In the profiles, we also compare the 1986–89 speeds with 1989–97 speeds. Values for the more recent pair are slightly lower, but within the estimated errors of the image-to-image cross-correlation technique. To improve data density for the mass flux calculation, we show a mean profile derived from combined data from all image pairs, and use this data to determine flow through the gates.

Mass flux through the Profile B gate is the integration of velocity times ice thickness across the width of the profile. Ice thickness data (from the BEDMAP 5 km ice thickness grid) ranges from 918 m to 1263 m, with a mean of 1177 m. Grid values in BEDMAP are similar to the nearest original values from German radio-echo sounding (Lambrecht *et al.* 1999). Further, the values are in very good agreement with thickness derived from ice elevation values just downstream of the grounding line (about 130 m). Using a seawater density of 1.028 g cm^{-3}, measured ice thickness is in agreement with measured ice elevation if the mean density of the ice column is 0.91 g cm^{-3}. We estimate the error in ice thickness to be no greater than 50 m, or about 4%. The sum of the flux across Profile B is 22.7 Gt a^{-1} (using a density conversion of 0.91 metric tons per cubic meter). Speed error, (± 15 m a^{-1} and ± 5 m a^{-1} for the older and newer image pairs, respectively) is approximately 2 to 6% of the mean speed. We conservatively estimate our overall flux error at about 10%, or ± 2 Gt a^{-1}. The flux value is similar to the InSAR-determined value of 23.7 ± 1.8 Gt a^{-1} (26.0 ± 2 km^3 times 0.91) reported in Rignot & Jacobs (2002).

Combining our catchment extent of 141 700 km^2 with the recent compilation of accumulation values provided by Vaughan *et al.* (1999) yields a snow input of 25.1 Gt a^{-1}; a compilation by Giovinetto & Zwally (2000) yields approximately 21.5 Gt a^{-1}. Both studies estimate that, on a regional scale (i.e. well above the scale of local undulations at 5 to 15 km), the compiled accumulation measurements are accurate to within ± 5%, or ± 1.3 Gt a^{-1}. In a recent survey of mass balance over the polar ice sheets Rignot & Thomas (2002) favoured the Giovinetto & Zwally (2000) values in data-sparse regions, which they believed yielded a more reasonable value for East Antarctic mass balance.

The two accumulation values bracket the mass balance point for IIS, given its calculated outflow. We derive a slightly positive net mass balance of 2.4 ± 4 Gt a^{-1} using the Vaughan *et al.* values, and a slightly negative balance of -1.2 ± 4 Gt a^{-1} using the Giovinetto & Zwally values, i.e. the glacier is in balance within errors of measurement. Further, IIS appears to be unchanging in flow speed at the present time. Additional evidence of stability comes from radar altimetry measurements of elevation in the northern catchment (north of -81.5°S, the extent of coverage). Observed elevation changes are low relative to those expected from snowfall variability (Wingham *et al.* 1998).

Driving stress and basal resistance to flow

By combining elevation and ice thickness from the RAMP DEM and the BEDMAP dataset, and comparing it with our image-derived velocity data, we can investigate the relationship of driving stress ($\rho g H \sin\alpha$, where ρ is density, g is gravitational acceleration, H is thickness and α is surface slope) with flow speed. This is a means of quickly

https://doi.org/10.1017/S0954102004001919 Published online by Cambridge University Press

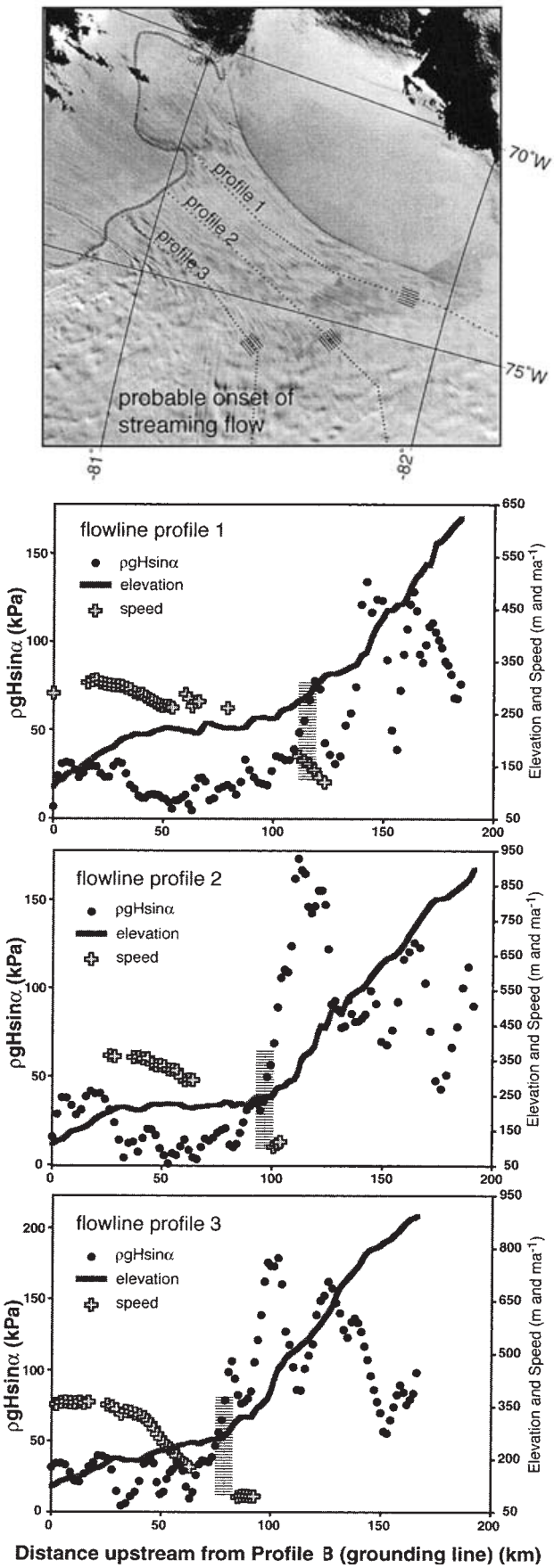


Fig. 6. Elevation, velocity, and driving stress for three along-flow profiles on IIS. Elevation data is derived from the RAMP DEM (Liu *et al.* 1999, Jezek *et al.* 2000). Velocity vectors are plotted when they lie within 1 km of the flow profile (roughly equal to one ice thickness). For the driving stress profiles, H (thickness) is derived from the BEDMAP compilation (Lythe *et al.* 2001) and local mean slope is determined by smoothing the RAMP DEM elevation profile at a spatial scale equivalent of 8 km. The hatchured bands in the image and profiles marks the inferred onset of streaming flow.

identifying regions of probable changes in basal conditions (e.g. Price *et al.* 2001). Figure 6 shows three along-flow profiles of IIS, plotting extracted data from the three datasets. Elevation profiles are derived from RAMP DEM data smoothed to 8 km spatial scale (approximately five times the local ice thickness). They show a pattern of steeper slope in the upper catchment area (~ 0.006), very low slopes in the main trunk (~ 0.0008), and then a short zone of steeper slopes near the grounding zone (~ 0.004). Thickness (not shown) varies only slightly compared to the large slope changes, and so the slope term dominates the driving stress variations. Velocity data (all vectors within 1 km of the profiles) shows the increasing speed along each of the flowlines. Hatched areas, plotted on both the image and the profiles, indicates regions where driving stress drops markedly as speed increases. The most plausible explanation for this pattern is a sharp drop in the mean basal resistive stress, suggesting a profound change in basal conditions and marking the 'onset' of primarily 'streaming', low-internal-deformation, flow.

Streakline morphology on the adjacent Ronne Ice Shelf

Streaklines result from flow over features in the bed, and are in general aligned parallel to ice flow in the grounded portions of ice streams and glaciers (except those with rapidly time-varying flow such as surging glaciers). Once transferred to floating ice, they serve as a recorder of flow direction and flux variation (see Fahnestock *et al.* 2000, Hulbe & Fahnestock in press). If streaklines are everywhere parallel to the flow direction in an ice shelf, it is powerful evidence that shelf flow direction and flux volume have been constant for the time required for ice to flow from the grounding line to the shelf front.

The enhanced-resolution AVHRR image in Fig. 1 shows the general streakline pattern in the Ronne Ice Shelf downstream from IIS and adjacent glaciers. The majority of outflow (approximately 75%) heads north-west from the grounding line and passes west of Korff Ice Rise. The remainder flows between Korff and Henry ice rises, across Doake Ice Rumples. However, on the southeast corner of Korff Ice Rise, the streaklines coming from IIS are folded. A close-up of this area is shown in an enhanced MODIS

https://doi.org/10.1017/S0954102004001919 Published online by Cambridge University Press

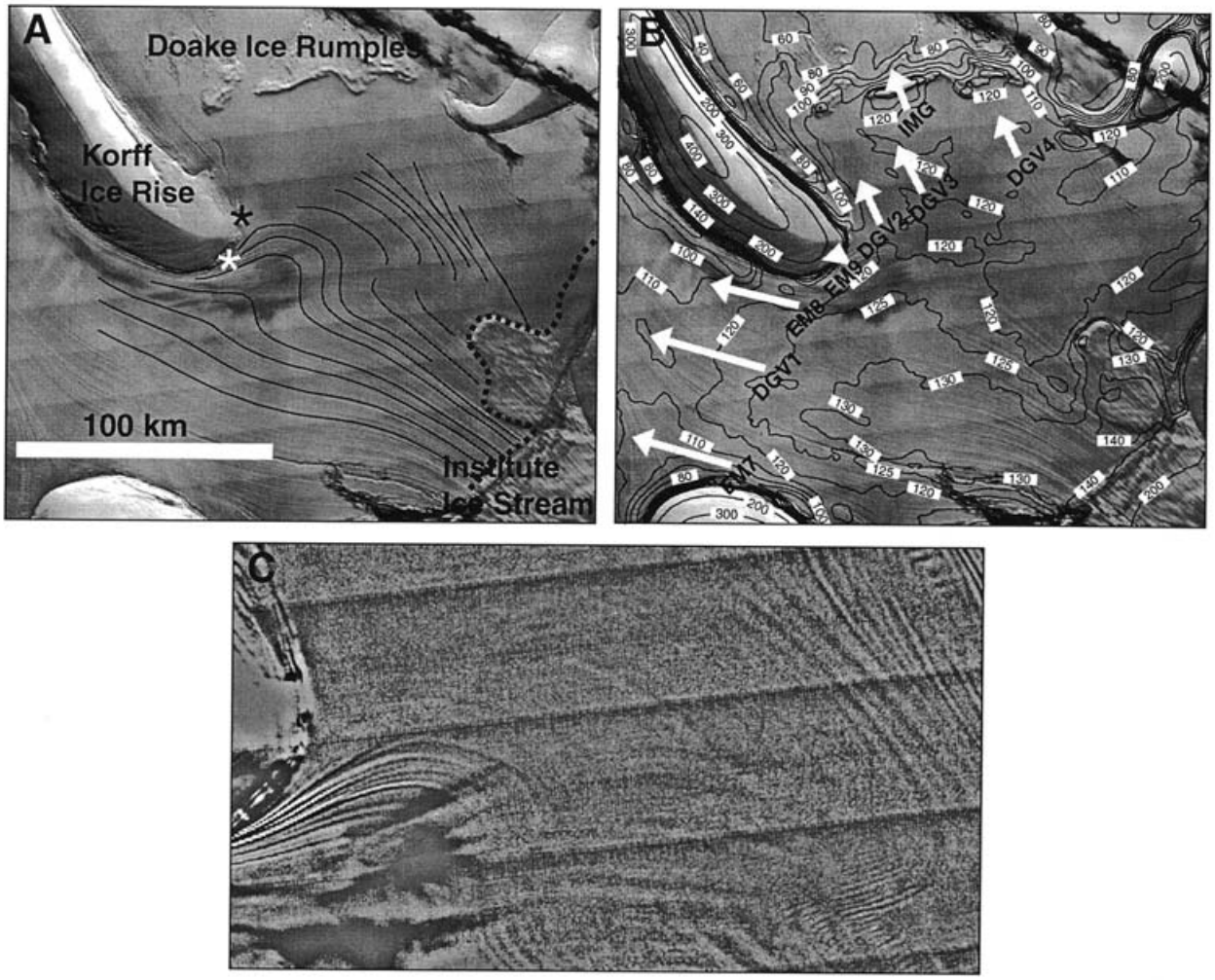


Fig. 7. Streaklines (A) and shelf ice elevations and velocities (B) plotted over an enhanced MODIS image of the outflow area of the Institute. An excerpt of the highly enhanced satellite image used for interpretation is shown in (C). Elevations are in meters above the OSU91A geoid. For vector scale, DGV1 represents 184 m a^{-1}; DGV2 is 67 m a^{-1}, and EM9 is 20 m a^{-1}. The vector IMG represents a cluster of closely spaced vectors of similar magnitude (all near 53 m a^{-1}) determined from image feature tracking. Shelf velocity data are from Vaughan & Jonas (1996). Asterisks in (A) represent flow divides around Korf ice rise, present (white) and past (black).

image as part of Fig. 7, along with ice velocity vectors from Vaughan & Jonas (1996) and detailed elevation data from photoclinometry.

The loop in the streaklines shown in Fig. 7 suggests a significant, recent rearrangement of flux between the east and west sides of Korff Ice Rise, with the eastern side acquiring a greater proportion of the net outflow. The location of the inferred 'split' in outflow around Korff Ice Rise has shifted to the left (viewed downstream) as more ice has turned toward the Doake Ice Rumples. The velocity vectors (Fig. 7b) show that ice flow is presently at a high angle to the streaklines, confirming that the present pattern is not steady-state. Elevation data shows the folded area is slightly higher, and presumably thicker, than the ice to the east. It also illustrates that elevations are much lower downstream of the Doake Ice Rumples, and that the westernmost rumple is lower than the others, rising only ~ 10 m above the shelf level versus ~ 20 m further east.

From the streakline pattern and present-day flow vectors, we have estimated the current and past flow divide location around Korff Ice Rise. This leads to a simple estimate of the magnitude of flux change over Doake Ice Rumples. Flow at survey point EM9 from Vaughan & Jonas (1996) is to the east at 20 m a^{-1}, so the current divide is somewhere slightly to the west of there. For the past divide, the streakline pattern appears to diverge at a point presently about 15 km to the east of the present divide. Tracing these points back towards the grounding line suggests that approximately 10% of the grounding line outflow has shifted eastward around Korff Ice Rise. (For this tracing, the shelf vectors and Landsat vectors are used for the present-day point; for the past configuration, the streaklines are followed).

https://doi.org/10.1017/S0954102004001919 Published online by Cambridge University Press

Flow vectors and streaklines also permit a rough estimate of the length of time since the rearrangement of flow began. In Fig. 7a, the maximum north-eastward deviation of the central streaklines in the pattern is about 25 km. Vectors DGV2 and DGV3, both nearly perpendicular to the streaklines at present, have speed values of 67 and 75 m a^{-1}, respectively. One estimate of the time of flow rearrangement, then, is ~ 360 years. This estimate assumes that the flow shift was abrupt and did not change in magnitude or direction after the event.

Discussion and summary

IIS has some features consistent with unconsolidated sediments at its bed, a shallow sub-glacial trough if any, and some evidence of change in outflow in the adjacent shelf flowlines. These include an ice-on-ice shear margin, an extensive ice plain, a central trunk with low slope and driving stress but very high speed, and the curvilinear outflow streaklines noted above. Central trunk slope is significantly lower than most outlet glaciers (e.g. Byrd, 0.0074; Thwaites, 0.0092; Pine Island, 0.0050; Slessor, 0.0038; Lambert, 0.0083; Bindschadler (formerly ice stream D), 0.0017; all data from RAMP DEM). Large ice plains like that fronting Whillans Ice Stream are also unusual.

The source of these kinds of characteristics in the eastern Ross Embayment glaciers and elsewhere is the geology underlying the ice, specifically, the presence of poorly consolidated sediments and a water-lubricated till layer formed from them (e.g. Engelhardt *et al.* 1990, Blankenship *et al.* 2001). Indeed, there was an inference from the earliest geophysical mapping of IIS that this was the case in this region of the FRIS grounding line as well (Drewry *et al*. 1980). Further, the bedrock surface not deeply incised by the ice, and the regional slope of that surface is low, allowing an extensive, highly variable water system to develop, and allowing for complex interaction between sea level, floating ice, and sub-ice sediments.

We agree with the earlier work of Drewry *et al*. (1980) suggesting that IIS and adjacent areas have unconsolidated sediments; further, the low driving stress implies loose till and, probably, a sub-ice water system with near-lithostatic pressures. The apparent differences between the north-eastern and south-western portions of IIS may reflect sub-ice geology changes. At present, the geology beneath this area is poorly known. A measurement of the current thermal profile of the lower IIS trunk, and a sample of the till beneath it, may provide an assessment of the stability of its ice flow; that is, of its stage in the ice stream till model outlined in Tulaczyk *et al.* (2000). This would inform modellers of the likely future of ice drainage in the IIS catchment.

In the shelf area downstream from IIS, the ongoing rearrangement of ice flow (and the fact that ice flux does not appear to be changing) implies that there have been changes to the resistance to flow across the Doake Ice Rumples. The two plausible causes are erosion of the bedrock forming the rumples, or a thinning of the ice flowing over them. Ice rumples, being shelf ice flowing up and over bed obstructions that impinge on the shelf underside, are inherently sensitive indicators of shelf ice thickness change, and as such may be useful as climate indicators responding to changes in sub-shelf ocean temperatures. For example, one possible explanation for the change in outflow is increased sub-shelf melting upstream of Doake Ice Rumples. However, in the recent study by Rignot & Jacobs (2002), IIS had the lowest present melting rate at its grounding line of all Antarctic glaciers measured, and the FRIS ice streams in general (Evans, Carlson, Rutford, Recovery, and Slessor ice streams) had low melt rates. Thus erosion is the favoured hypothesis.

We suggest that a program of field study at IIS and adjacent areas would yield important information for glaciology, the past and future of ice flow in the region, and the regional geology. In particular, sampling of the bed in several locations (e.g. via hot-water drilling) could provide geologic samples, allowing comparison with geologic samples from other regions of rapid, low-driving stress, ice flow. A drill site at the Doake ice rumples might provide evidence of erosion there. Further, these sites would provide a means to determine the ice temperature profile, now recognized as critical to the initiation and cessation of streaming flow. Ice-penetrating radar profiling of the north-eastern margin would allow a structural comparison with similar profiles of other ice streams. Radar profiling of the adjacent dome (Bungenstock ice rise), and of Korff Ice Rise, could provide information about the longer-term history of ice drainage through internal layer modelling.

Acknowledgements

A. Lambrecht kindly provided data from her dissertation study of the adjacent Ronne Ice shelf and Foundation Ice Stream. Ice velocity mapping and photoclinometry algorithms were developed in collaboration with Dr Mark Fahnestock. Dr Jonathan Bamber and an anonymous reviewer provided suggestions that streamlined the manuscript and refined its focus, as did editor Michiel van den Broeke. This work was funded by two grants from NASA, supporting Antarctic applications of Landsat data (NAG5-3438) and photoclinometry of ice sheets (NAG5-7760).

References

ALBERTS, F.G. 1995. *Geographic names of the Antarctic*. 2nd ed. Washington: US Department of the Interior, 834 pp.

BAMBER, J.L., VAUGHAN, D.G. & JOUGHIN, I. 2000. Widespread complex flow in the interior of the Antarctic ice sheet. *Science,* **287**, 1248–1250.

https://doi.org/10.1017/S0954102004001919 Published online by Cambridge University Press

BINDSCHADLER, R.A. 1998. Monitoring ice-sheet behavior from space. *Reviews of Geophysics,* **36**, 79–104.

BINDSCHADLER, R.A. & SCAMBOS, T.A. 1991. Satellite-image-derived velocity field for an Antarctic ice stream. *Science,* **252**, 242–246.

BINDSCHADLER, R.A. & VORNBERGER, P.L. 1994. Detailed elevation map of Ice Stream C, Antarctica using satellite imagery and airborne radar. *Annals of Glaciology,* **20**, 327–335.

BLANKENSHIP, D.D., MORSE, D.L., FINN, C.A., BELL, R.E., PETERS, M.E., KEMPF, S.D., HODGE, S.M., STUDINGER, M., BEHRENDT, J.C. & BROZENA, J.M. 2001. Geologic controls on the initiation of rapid basal motion for West Antarctic ice streams: a geophysical perspective including new airborne radar sounding and laser altimetry results. *Antarctic Research Series,* 77, 105–121.

DOAKE, C.S.M. 1987. Some aspects of the flow of the Ronne Ice Shelf. *In* VAN DER VEEN, C.J. & OERLEMANS, J., *eds*. *Dynamics of the West Antarctic Ice Sheet*. Dordrecht: Reidel, 75–98.

DREWRY, D.J., MELDRUM, D.T. & JANKOWSKI, E. 1980. Radio echo and magnetic sounding of the Antarctic Ice Sheet, 1978–79. *Polar Record,* **20**, 43–57.

DREWRY, D.J. *ed*. 1983. *Antarctica: glaciological and geophysical folio.* Cambridge: Scott Polar Research Institute.

ENGELHARDT, H., HUMPHREY, N., KAMB, B. & FAHNESTOCK, M. 1990. Physical conditions at the base of a fast-moving Antarctic ice stream. *Science,* **248**, 57–59.

FAHNESTOCK, M.A., SCAMBOS, T.A., BINDSCHADLER, R.A. & KVARAN, G. 2000. A millennium of ice flow variation recorded by the Ross Ice Shelf. *Journal of Glaciology,* **46**, 652–664.

GIOVINETTO, M. & ZWALLY, J. 2000. Spatial distribution of net surface accumulation on the Antarctic ice sheet. *Annals of Glaciology,* **31**, 171–176.

GRAY, A.L., SHORT, N., MATTAR, K.E. & JEZEK, K.C. 2001. Velocities and flux of the Filchner Ice Shelf and its tributaries determined from speckle tracking interferometry. *Canadian Journal of Remote Sensing,* **27**, 193–206.

HARAN, T., FAHNESTOCK, M. & SCAMBOS, T.A. 2002. De-striping of MODIS optical bands for mapping and topography. *EOS,* 83(47), F317.

HULBE, C.L. & FAHNESTOCK, M.A. In press. West Antarctic ice stream discharge variability: mechanism, controls, and pattern of grounding line retreat. *Journal of Glaciology*.

JEZEK, K. 1999. Glaciological properties of the Antarctic ice sheet, from Radarsat-1 Synthetic Aperture Radar Imagery. *Annals of Glaciology*, **29**, 286–290.

JEZEK, K., LIU, H., ZHAO, Z. & LI, B. 1999. Improving a digital elevatoin model of Antarctica using radar remote sensing data and GIS techniques. *Polar Geography*, **23**, 185-200.

JOUGHIN, I.L., GRAY, L., BINDSCHADLER, R., PRICE, S., MORSE, D., HULBE, C., MATTAR, K. & WERNER, C. 1999. Tributaries of West Antarctic ice streams revealed by RADARSAT interferometry. *Science,* **286**, 283–287.

LAMBRECHT, A., MAYER, C., OERTER, H. & NIXDORF, U. 1999. Investigations of the mass balance of the southeastern Ronne Ice Shelf, Antarctica. *Annals of Glaciology,* **29**, 250–254.

LIU, H., JEZEK, K.C. & LI, B. 1999. Development of an Antarctic digital elevation model by integrating cartographic and remotely sensed data: a geographic information system based approach. *Journal of Geophysical Research,* **104**, 23199–23214.

LYTHE, M.B., VAUGHAN, D.V. & THE BEDMAP CONSORTIUM. 2001. BEDMAP: a new ice thickness and subglacial topographic model of Antarctica. *Journal of Geophysical Research,* **106**(B6), 11335–11351.

MCINTYRE, N. 1986. Discharge of ice into the Filchner-Ronne Ice Shelves. *In* KOHNEN, H., *ed*. *Filchner-Ronne-Ice-Shelf-Programme,* 3. Bremerhaven: Alfred-Wegner-Institute for Polar and Marine Research, 47–52.

PRICE, S., BINDSCHADLER, R., HULBE, C. & BLANKENSHIP, D. 2001. Force balance along a tributary and onset to Ice Stream D. *Journal of Glaciology*, **48**, 20–30.

RIGNOT, E. & JACOBS, S.S. 2002. Rapid bottom melting widespread near Antarctic ice sheet grounding lines. *Science*, **296**, 2020–2023.

RIGNOT, E. & THOMAS, R.H. 2002. Mass balance of polar ice sheets. *Science*, **297**, 1502–1506.

SCAMBOS, T.A., DUTKIEWITCZ, M.J., WILSON, J.C. & BINDSCHADLER, R.A. 1992. Application of image cross-correlation software to the measurement of glacier velocity using satellite image data, *Remote Sensing of Environment*, **42,** 177–186.

SCAMBOS, T.A. & FAHNESTOCK, M.A. 1998. Improving digital elevation models over ice sheets using AVHRR-based photoclinometry. *Journal of Glaciology*, 44, 97–103.

SCAMBOS, T.A., KVARAN, G. & FAHNESTOCK, M.A. 1999. Improving AVHRR resolution through data cumulation for mapping polar ice sheets. *Remote Sensing of Environment*, 69, 56–66.

SCAMBOS, T.A. & HARAN, T. 2002. An image-enhanced DEM of the Greenland ice sheet. *Annals of Glaciology*, **34**, 291–298.

SWITHINBANK, C., BRUNK, K. & SIEVERS, J. 1988. A glaciological map of Filchner-Ronne Ice Shelf, Antarctica. *Annals of Glaciology*, **11**, 150–155.

TULACZYK, S., KAMB, W.B., & ENGELHARDT, H.F. 2000. Basal mechanics of Ice Stream B, West Antarctica 2. Undrained plastic bed model. *Journal of Geoplysical Research*, **105**(B1), 483–494.

VAUGHAN, D.G., BAMBER, J.L., GIOVINETTO, M.B., RUSSELL, J. & COOPER, A.P.R. 1999. Reassessment of net surface mass balance in Antarctica. *Journal of Climate*, **12**, 933–945.

VAUGHAN, D.G. & JONAS, M. 1996. Measurements of velocity of Filchner-Ronne Ice Shelf. *In* OERTER, H., *ed. Filchner-Ronne Ice Shelf Programme (FRISP) Report* No.10. Bremerhaven: Alfred Wegner Institute, 111–118.

VAUGHAN, D.G., SMITH, A.M., CORR, H.F.J., JENKINS, A., BENTLEY, C., STENOIEN, M.D., JACOBS, S.S., KELLOGG, T.B., RIGNOT, E. & LUCCHITTA, B. 2001. A review of Pine Island Glacier, West Antarctica: hypotheses of instability versus observations of change. *Antarctic Research Series*, **77**, 237–256.

WINGHAM, D., RIDOUT, A.J., SCHARROO, R., ARTHERN, R. & SHUM, C.K. 1998. Antarctic elevation change from 1992 to 1996. *Science*, **282**, 456–458.

https://doi.org/10.1017/S0954102004001919 Published online by Cambridge University Press